Известия Уральского государственного горного университета. 2019. Вып. 1(53). С. 7-17

Науки о Земле
Earth sciences

УДК 550.83

https://doi.org/10.21440/2307-2091-2019-1-7-17

Basement configuration depth methods of airborne magnetic data in the eastern Gulf of Suez, Egypt

Sergey Vladimirovich SHIMANSKIY[1, *],
Ahmed TARSHAN[1, 2, **]

[1]Saint Petersburg State University, Saint Petersburg, Russia
[2]Nuclear materials Authority, Cairo, Egypt

One of the best methods used to delineate basement structures and configuration is the airborne magnetic survey data.
The goal of this research is to accurately delineate the deep-seated basement configuration and structures. Production of geophysical maps after processing the data, including two-dimensional (2D) and three-dimensional (3D) magnetic susceptibility layered-earth models for high-resolution airborne RTP magnetic data over the eastern part of the Gulf of Suez, was conducted to accurately detect the shallow and deep-seated basement structures. The well data was used to correlate and control the depth of the basement during the 2D and 3D modelling.
Results of the estimation of the depth to the basement showed that Analytical Signal (AS), Source Parameter Imaging (SPI) and Euler methods have very similar results. The eastern part in the three maps indicates more shallow depths that reach 300 m in some locations; on the other hand, the western part of the area indicates deeper depths to the basement, which in some places reaches 5000 m from the existing averaged ground surface. The 3D modelling showed an adequate matching between the depth to the basement in the calculated and observed data. The sedimentary section is tectonically affected by such deep-seated basement structures with a set of faults that extend from the basement upwards through the sedimentary cover. Generally, these faulted sedimentary blocks may constitute potential structural traps for the hydrocarbon accumulation.

Keywords: 2D and 3D magnetic susceptibility, layered-earth models, deep-sated basement structures, regional and residual RTP, eastern Gulf of Suez region.

Introduction

The airborne magnetic tool method is one of the best methods used to illustrate the horizontal variation in magnetic properties of underlying rocks. Generally, the basement rocks represent deeper anomalies and have high magnetic fields, while the sedimentary rocks represent the shallower anomalies and have lower magnetic fields.

The oldest rocks in Egypt are basement rocks; these rocks have likely recorded all tectonic events that have affected Egypt since the beginning of the Cambrian period to the present. The aeromagnetic survey method is one of the most effective geophysical methods for mapping tectonic trends of deeply buried basement rocks. Usually, aeromagnetic mapping reflects the horizontal variation in magnetic properties of underlying rocks. In this regard sedimentary rocks, excluding iron ores and basic extrusions intruded within them, are characterised by very low magnetic susceptibility, while igneous and metamorphic rocks (the main components of basement rocks) are strongly magnetised. The more heterogeneous and deformed the basement rocks, the shaper and stronger their magnetic signatures will be on the aeromagnetic map [1].

In this research, different methods to determine the depth to the basement at the eastern part of the Gulf of Suez were applied. There are many methods that can be used to delineate the depth to the basement such as source parameter imaging (SPI), analytical signal method and Euler Method. Additionally, the role of three-dimensional (3D) modelling has become more important. The 3D modelling in geophysics is divided into two important parts: the forward and the inverse problem. In geophysics, for the forward problem, a model is given and the data is calculated, while geophysical inversion is mathematical technique used to retrieve information about sub-surface physical properties (magnetic susceptibility, density, electrical conductivity, etc.) of measured geophysical data.

The observed total magnetic intensity in the airborne magnetic survey is measured as a result of the Earth's Magnetic Field. The forward model has a unique solution in which the data is calculated depending on the model. However, when applying the inverse process the reasonable produced model depends on the measured data. The main factor that controls the observed magnetic field on the earth's surface is the susceptibility differences distribution (Δk) in the subsurface.

The main target of the inverse process is to minimize the deviation between the measured and calculated data. Usually an iterative procedure is used to reach this goal, where the data and model parameter vectors are related via a non-linear response function, which tells us how to calculate the synthetic data from the given model.

Data acquisition

During March 1998, the Airborne Geophysics Department of the Nuclear Materials Authority (NMA) of Egypt led a high-resolution aeromagnetic survey covering 2745 km^2 over the eastern part of the Gulf of Suez. Data was gained along primary

*s.shimanskii@spbu.ru
http://orcid.org/0000-0001-9710-9392
** ahmed_ramadan_geo@hotmail.com
http://orcid.org/0000-0002-5403-5220

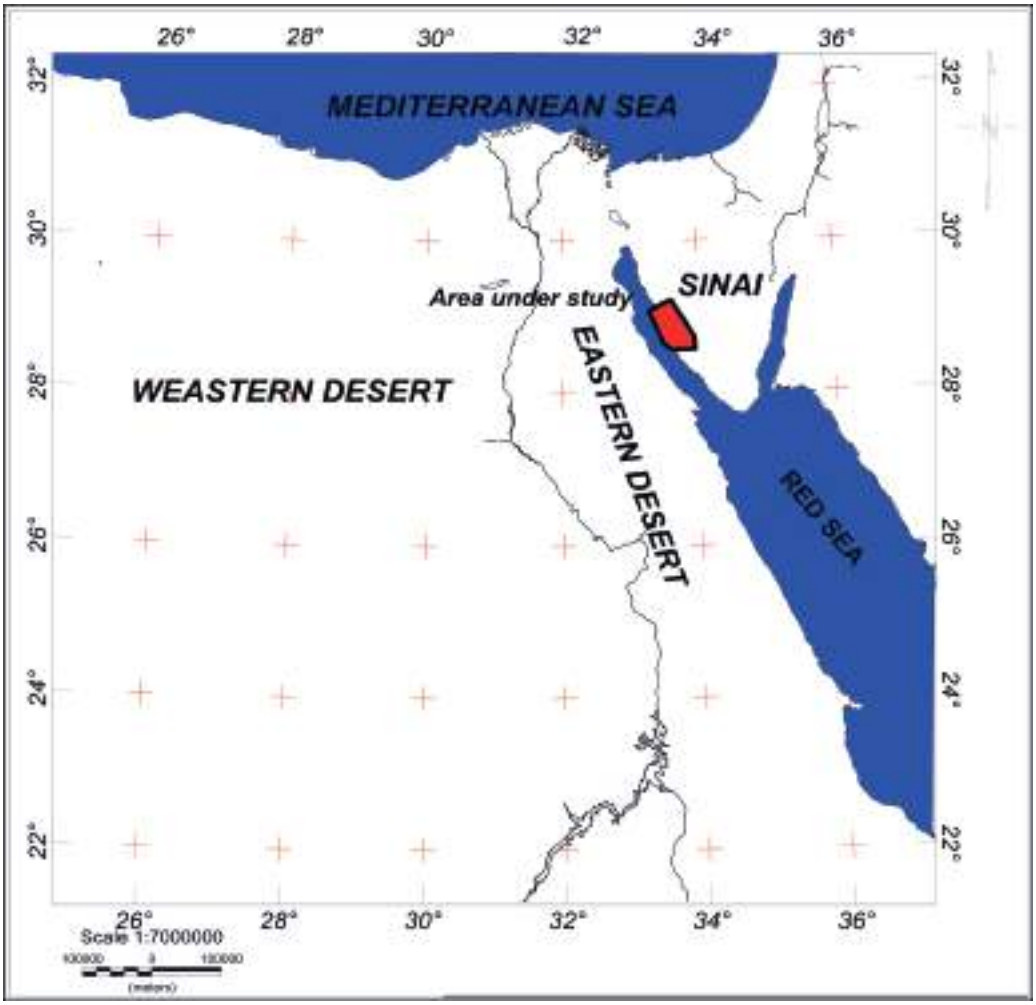

Figure 1. The map of Egypt showing the location of the area under study.
Рисунок 1. Карта Египта с указанием местоположения исследуемой территории.

(essential) lines spaced at 1000 m and along control lines spaced at 10000 m (normal to the primary lines). Nominal flying elevation was about 100 m (330 ft) above ground surface (terrain clearance). The direction of the survey was 125°–305° azimuth degrees for primary lines and 35°–215° azimuth degrees for control lines (Fig. 1).

Geologic features

Geologically, the area is covered by a variety of rock formation from Quaternary, Miocene, Paleocene, Cretaceous and Paleozoic Eras (Fig. 2). It contains man made features such as several oil fields (Rudeis, Feiran and Belayim oil fields). The western side of the studied area is part of the Gulf of Suez. It is dominated by several mountains such as Gabal Zeit at the southern part of the area, which is formed of undeformed alkali granitic rocks, Gabal Nazzazat (formed of siliciclastic- carbonate succession) and Gabal Ekmain the central part of the area. There are some Wadis within the area such as Wadi Abu Ratamat, Wadi Abiad and Wadi Thaghada. The nearby eastern part of the Gulf of Suez is covered by Quaternary deposits (Fig. 2).

Airborne magnetic data calibration and processing

The Figure of Merit (FOM) test, heading test and lag test were applied after the survey. The FOM test was carried out at flight height 10,000 above sea level at each survey direction. Heading test was carried out. The values of the heading used in the processing of the data are ± 10 and ± 6 for primary lines and tie lines, respectively. The lag test was applied to establish the magnitude of any timing differential within the whole survey system. The resulting parallax/lag error calculated was 0.6 seconds. The magnetometer base station was used to remove the diurnal variation twice daily before and after survey, rather than repeated flying on control lines across the traverse lines. The data was obtained from the fixed magnetometer (magnetometer base station) used in correcting the observed data by direct subtraction.

The International Geomagnetic Reference Field (IGRF) correction is done to remove the regional gradient of the Earth's Magnetic Field due to the continual changes in the direction and magnitude of the earth's main field as one goes from one place to another [3]. The magnetic field of the earth is recorded every five years as international magnetic map. Data levelling and Micro levelling applications were applied. The origin of levelling problems is that geophysical surveys collect data under constantly changing conditions that contribute to errors. The most obvious effect of such errors is an apparent level shift in neighbouring parallel survey lines, which is a phenomena commonly referred to as levelling error.

Systematic errors are measurable and can be corrected using simple mathematical formulae and systematic corrections compensate for measurable errors in the data. Systematic errors follow regular patterns and are removed mathematically by the computer [4].

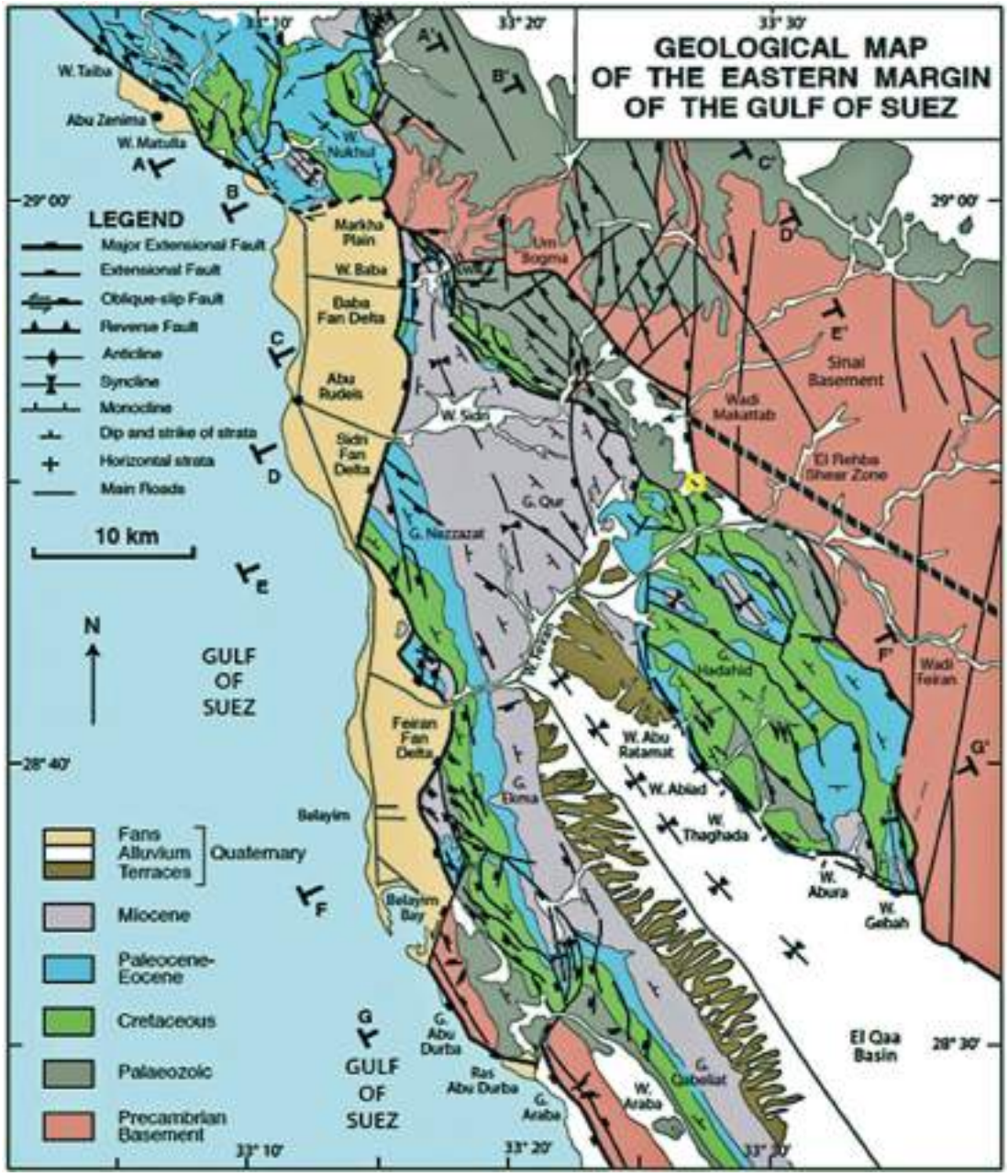

Figure 2. Geological map of the Middle Eastern part of the Gulf of Suez, Egypt [2].
Рисунок 2. Геологическая карта средневосточной части Суэцкого залива, Египет [2].

Data treatment and qualitative/semi-qualitative analysis

Three filled-colour contour maps were created from the aerial magnetic survey data. The reduced to the pole (RTP) map (Fig. 3) is generated from a total magnetic intensity map. Because of the inclination of the earth's magnetic field, most magnetic anomalies show both positive and negative counterparts. These minimum and maximum anomalies are generally displaced from the centre of the causative body along the magnetic meridian line. This is only the case when the inclination is 90° and the magnetic anomaly lies directly over the centre of the source body. The RTP is used to remove this effect, so that the data appears as if observed at the pole where the magnetic field is vertical. The magnetic peaks, then, occur directly over the magnetised bodies, particularly in the case of absence of remnant magnetization [5]. In the opposite case, when the inclination is equal to 0°, the minimum is located directly over the magnetic body. The field reduced to the pole at a fixed point above the measurement plane in the frequency domain is given by [6]

$$L(\theta) = 1/[\sin(I_a) - i\cos(I)\cos(D+\theta)]^2, \text{ if } (I_a < I),\ I_a = I,$$

where I – geomagnetic inclination, I_a – inclination for amplitude correction (never less I); D – geomagnetic declination, θ – wave number direction, i – imaginary component.

Regional and residual magnetic-component maps, which are created by the Gaussian filter technique (Fig. 4, a, b), are produced. The separation processes are designed to separate broad deeper variations "i. e., regional" from sharper local variations "i. e., residual" magnetic anomalies. In other words, the magnetic map is split into two parts, the regional and the residual

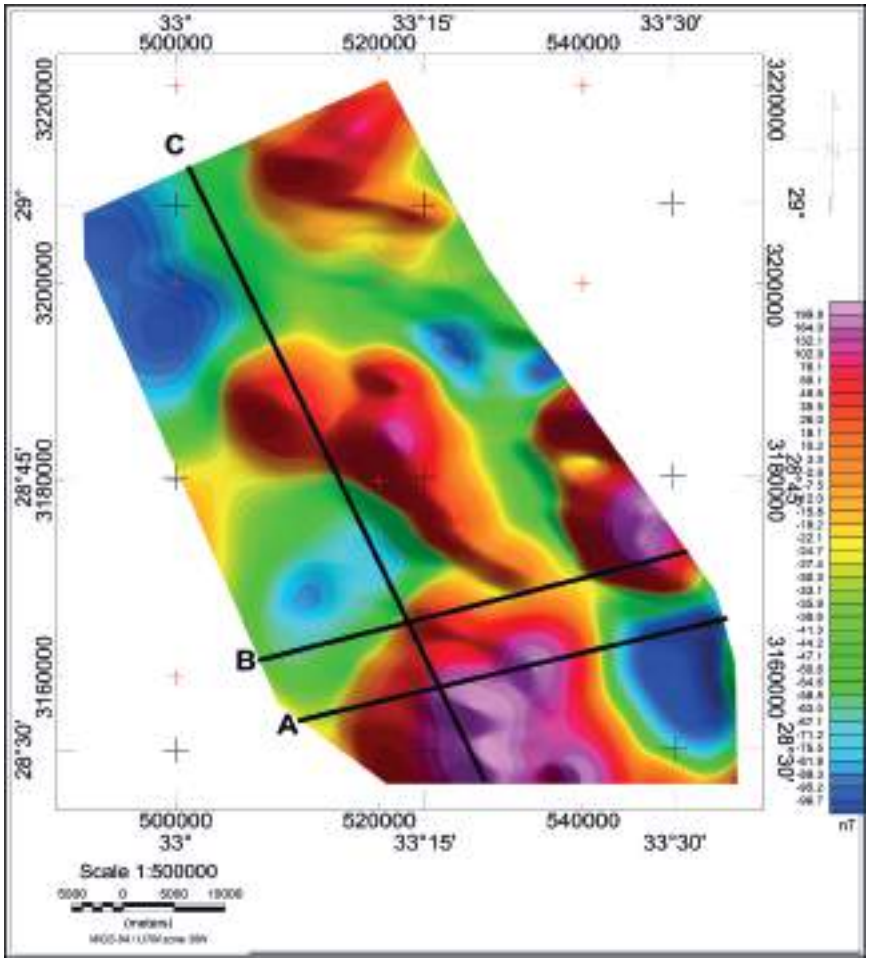

Figure 3. Colour shaded contour map of Reduced to North Pole Total Magnetic Intensity Field showing the profiles of the two-dimensional modelling, eastern part of the Gulf of Suez, Egypt.
Рисунок 3. Цветная контурная карта полного вектора магнитного поля, редуцированного к Северному полюсу, показывающая профили двухмерного моделирования (восточная часть Суэцкого залива, Египет).

magnetic-component maps. The residual map focuses map attention on weaker features, which are obscured by strong regional effects on the original map [7].

The energy (power) spectrum

The calculated radially averaged power spectrum (Fig. 5) for the aeromagnetic RTP can be divided into three portions. The first one represents regional or deep sources components that are in the frequency range of 0.0 to 0.15 cycles per km. The second portion represents residual or shallow sources components that range in frequency from 0.15 to 0.65 cycle/km. The third portion, which frequency exceeds 0.65 cycle/km, is the noise component. The estimated mean depths of both regional and residual sources were found to be 4.5 km and 1.8 m, respectively (Fig. 4).

Magnetic depth estimation

Magnetic data analysis was used to guide the structural configuration and composition of the basement using three advanced techniques. These methods are analytical signal (AS), source parameter imaging "SPI" and Euler method [8].These methods have proved to be effective tools for locating magnetic structures such as faults.

A. Analytical signal (AS) technique

The analytical signal is the square root of the sum of the squares of the vertical and the two horizontal derivatives of the total magnetic field. The analytical signal approach has been successively used in the form of 3D interpretation of aeromagnetic data [9].

The analytical signal method's success results from the fact that the location and depth of magnetic sources are found with only a few assumptions about the nature of the source body, which is typically assumed as a two-dimensional (2D) magnetic source such as contact, step, horizontal cylinder and dike. The amplitude shape of the analytical signal for these geological models is a bell-shaped symmetric function located directly above the source body. The magnetic source depths, using the magnetic method, are calculated from the ratio of the total magnetic analytical signal to the vertical derivative analytical signal of the total magnetic intensity (Fig. 6, a).

B. Source Parameter Imaging (SPI) technique

SPI is a technique based on the extension of complex analytical signals to calculate magnetic depths [8]. The interference and overlap of anomaly features is reducible due to using second-order derivatives in this method. The method is used on gridded data by first estimating the direction at each grid point. The vertical gradient is calculated in the frequency domain, and the horizontal derivatives are calculated in the direction perpendicular to the strike using the least-squares method (Fig. 6, b).

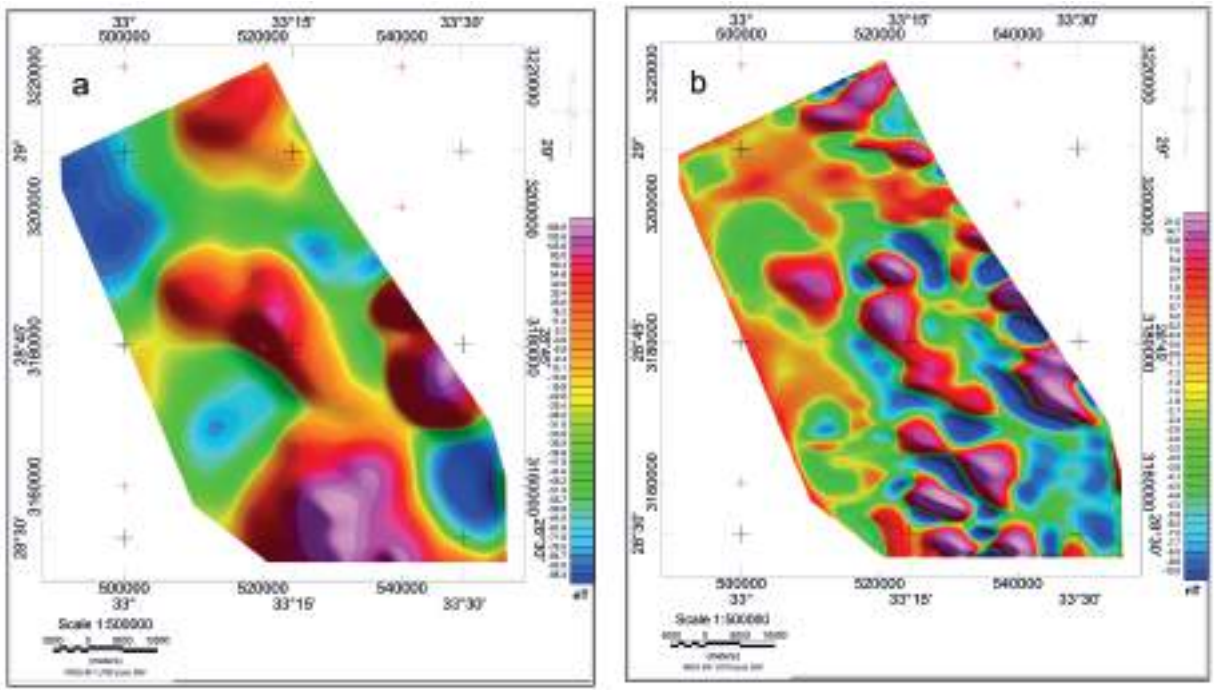

Figure 4. Colour shaded contour map of a) the regional and b) the residual magnetic components of the RTP map eastern part of the Gulf of Suez, Egypt.
Рисунок 4. Цветная контурная карта а) региональной и б) остаточной магнитной компоненты, редуцированной к полюсу карты, восточной части Суэцкого залива, Египет.

C. Euler method

Euler deconvolution method is an advanced technique depending on both amplitude and gradients to determine the source of potential fields. At first, this method was used to interpret the 2D magnetic anomalies, developed to be used on grid-based data. Magnetic field M and its spatial derivatives satisfy Euler's equation of homogeneity (Fig. 6, c), this method was developed by Thompson [10]

$$\left(x-x_0\right)\frac{\partial M}{\partial x}+\left(y-y_0\right)\frac{\partial M}{\partial y}+\left(z-z_0\right)\frac{\partial M}{\partial z}=-NM,$$

where $\frac{\partial M}{\partial x}$, $\frac{\partial M}{\partial y}$ and $\frac{\partial M}{\partial z}$ represent first order derivatives of the magnetic field along the x, y and z directions, respectively; N is the structural index and is related to the geometry of the magnetic source. For example, $N = 0$ for magnetic contact, $N = 1$ for thin dike, $N = 2$ for pipe and $N = 3$ [11].

The first look at the three maps shows that AS, SPI and Euler methods have very similar results (Fig. 6, a–c).The eastern part in the three maps indicates more shallow depths to the basement that reach 300 m in some locations. On the other hand, the western part of the area indicates deeper depths to the basement, which in some locations reaches 5000 m. The central southern part of the area in the three maps refers to the existence of the basement at very low depths, where in some places the depth to the basement in the area is outcropped. On the other hand, the depths become greater moving towards the east, which may be evidence of the existence of a basin. The result of the depths to the basement of the analytical signal method ranges from115 to 5000 m and the depths to the basement of the SPI method ranges from 384 to 5134 m, while the depths obtained from Euler method vary from 414 to 5177 m. The results of the three methods are very similar to each other.

Two-dimensional (2D) data inversion

2D inverted susceptibility layered-earth model was applied along three profiles within the area under study as shown in (Fig. 3).

Profile A (Fig. 7), extends more than 42 km long in the SW-NE direction passing through Well Belayim Bay-3 [12], which controls the geometry and physical parameters of the basement blocks. The depth at this well showed great compatibility between real and calculated depth, which is equal to 3530 m.

This profile shows a good fit between the observed and calculated magnetic curves with root mean square (RMS) equal 2.582%. The type of basement rock from different wells within the area is granite. The magnetic susceptibility used at this profile is 0.0045 SI. The moderate thick sedimentary layer with varying thickness overlaying the basement rocks has an average susceptibility value. The depth to the basement in the middle of the profile is shallower than the depth at the edges, where the depth at the eastern part is more than 6000 m, which matches with AS and SPI maps (Fig. 6, a, b). Structurally, the profile shows that the basement is tilted by a number of normal faults where the main trend of the extension stress pattern of the gulf is in a NE-SW direction.

Profile B, extends more than 42 km, passing through Belayim 112-64 well [12], which controls the geometry and physical parameters of the basement blocks. The depth at this well showed great compatibility between real and calculated depth, which is equal to 2285 m. This profile shows an excellent fit between the observed and calculated magnetic curves with RMS equal to

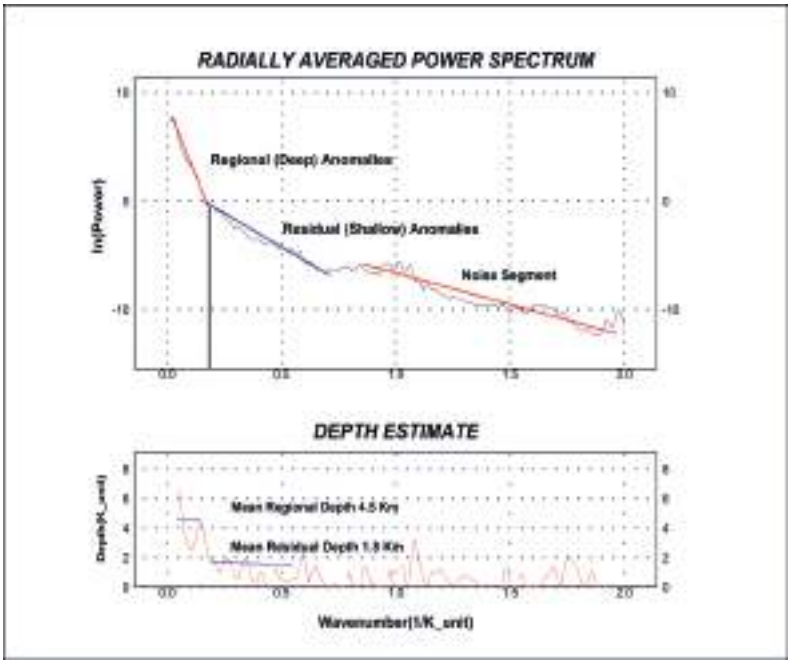

Figure 5. Power spectrum of magnetic data showing the corresponding averaging depths, eastern part of the Gulf of Suez, Egypt.
Рисунок 5. Спектр мощности магнитных данных, иллюстрирующий соответствующие усредняющие глубины (восточная часть Суэцкого залива, Египет).

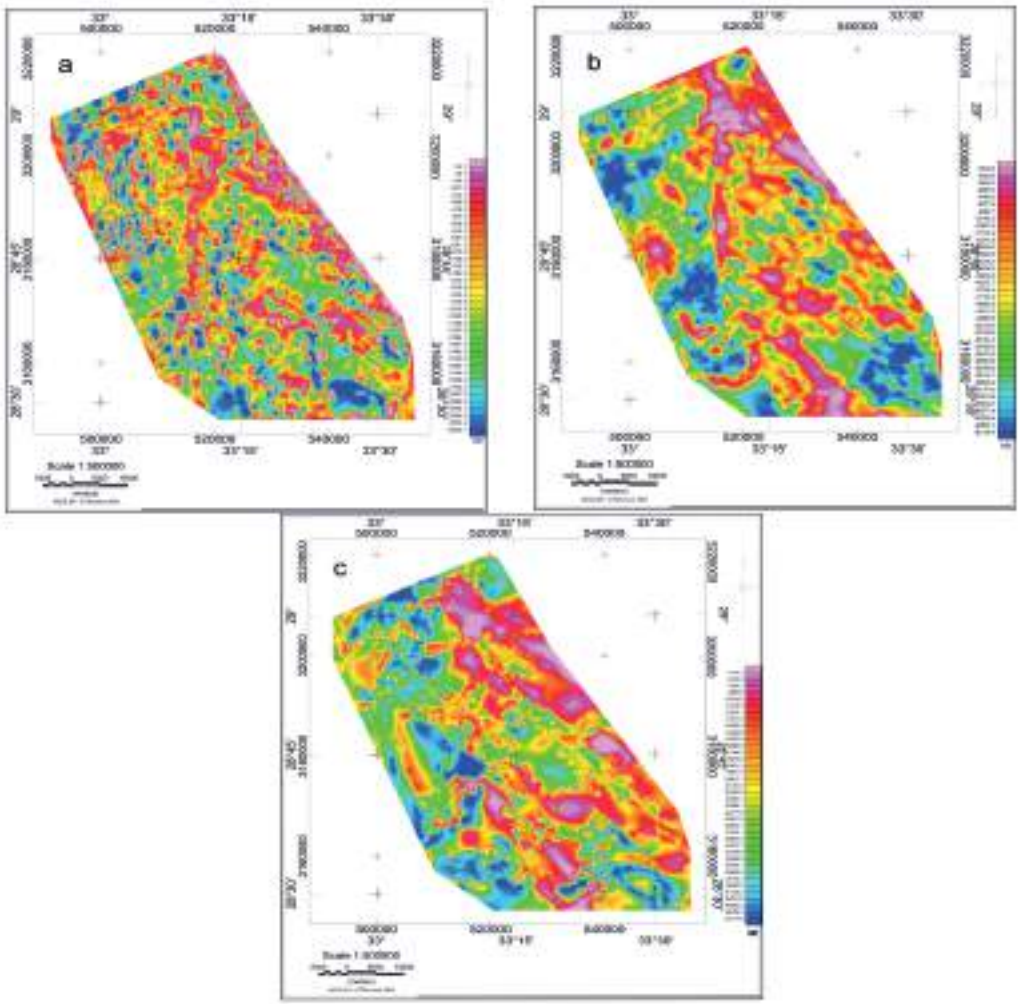

Figure 6. Filled colour contour map of depth to magnetic bodies as calculated using a) analytical signal method, b) source parameter imaging (SPI) and c) Euler Method, eastern part of the Gulf of Suez, Egypt.
Рисунок 7. Закрашенная контурная карта глубин до магнитных тел согласно вычислениям с использованием а) метода аналитического сигнала, б) изображения источникового параметра и в) метода Эйлера (восточная часть Суэцкого залива, Египет).

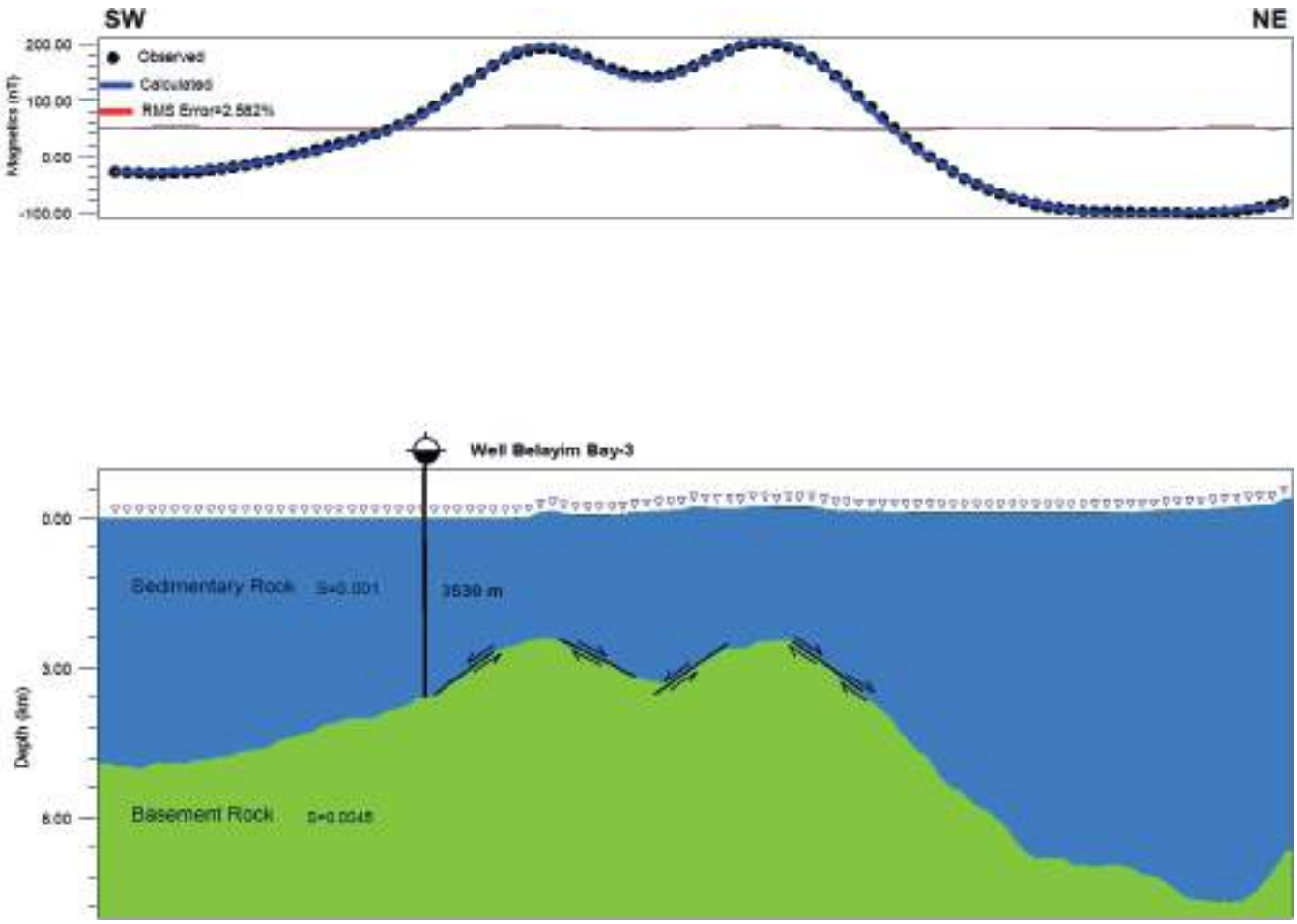

Figure 7. 2D inverted susceptibility layered-earth model and calculated geomagnetic response of the profile A, eastern part of the Gulf of Suez, Egypt.
Рисунок 7. Двухмерная модель магнитной восприимчивости, полученная решением обратной задачи для слоистой земли, и вычисленный геомагнитный отклик профиля А (восточная часть Суэцкого залива, Египет).

2.525%. The magnetic model proved the presence of a moderate sedimentary layer in the north western part of the profile, which has an average susceptibility value of 0.001 SI that decreases to the north east because the depth to the basement decreases close to the Precambrian outcropped basement of Sinai. Structurally, the profile shows that the basement is tilted by a number normal faults formed due to tension forces in the NE and SW direction.

Profile C (Fig. 8), extends more than 68 km long in the NW-SE direction. This profile shows an excellent fit between the observed and calculated magnetic curves with RMS equal to 3.233%. This profile passes through three wells that are used to control the depth to the basement Abu Zeneima 11-1s1, Feiran N.-1 and Belayim 112-64 [12]. The depth at this well showed great compatibility between real and calculated depth, which is equal to 3830, 3825, and 2285 m, respectively. Structurally, the profile shows that the basement is tilted by a number of normal faults. The depth to the basement becomes shallower at the south western part than the north eastern part. This is evidence for existence of a basin in the northern part of the area.

3D magnetic modelling interpretation

Using GM–SYS–3D inversion code, the presumed sedimentary section–basement complex magnetic susceptibility contrast Δk for several inversion trials was gradually set between 0.035 and 0.08 SI during the inversion run. The inverted basement relief images, corresponding to the used susceptibility contrasts, were consistently inspected. The effective susceptibility contrast was found close to the susceptibility contrast of 0.0628 SI (5000 micro cgs unit), and correspondingly its calculated basement relief image (Fig. 9). The overall calculated 3D response fit the observed geomagnetic data better than ±50.0 nT. Other model parameters are set to be constant for all trails (convergence limit: 10 nT, Z0: 0 m and regional offset: 0.0), where Z0 is the nominal top of basement surface.

The depth to the basement estimates reliably varied between 500 and 4700 m. The depth to the basement correlated with the available drilled stratigraphic-control wells within the area under study. These wells are RB-A5 [13], Abu Zeneima 11-1S1 and Feiran N-1 [12], BM 113-27 [14], Ekma-1 and Abu-Durba 115-1 [15]. The encountered basement relief at the study area was shown up with three major basinal structures. These basins are located at the north western, central western and south eastern part of the area.

The available wells were sufficient to some extent to constrain the inversion process but if more wells are available they could help in constraining the inversion and minimising the misfit value. At the unconstrained location, the misfit value is higher and error could be because of the variation in magnetic susceptibility of the basement. The depths to the basement at the available wells in the calculated basement relief image showed a good matching with the actual values of the depths at these wells. Table shows the actual and observed value of depth to basement at each well.

Calculated and actual depth at the available wells within the area under study.
Расчетная и фактическая глубина на имеющихся скважинах в пределах исследуемой территории.

Well Number	Well Name	Calculated Depth (m)	Actual Depth (m)
1	RB-A5	3765	3761
2	Abu Zeneima 11-1s1	3850	3830
3	Feiran N-1	3830	3825
4	BM 113-27	4189	4181
5	Ekma-1	2174	2170
6	Abu-Durba 115-1	2091	2090

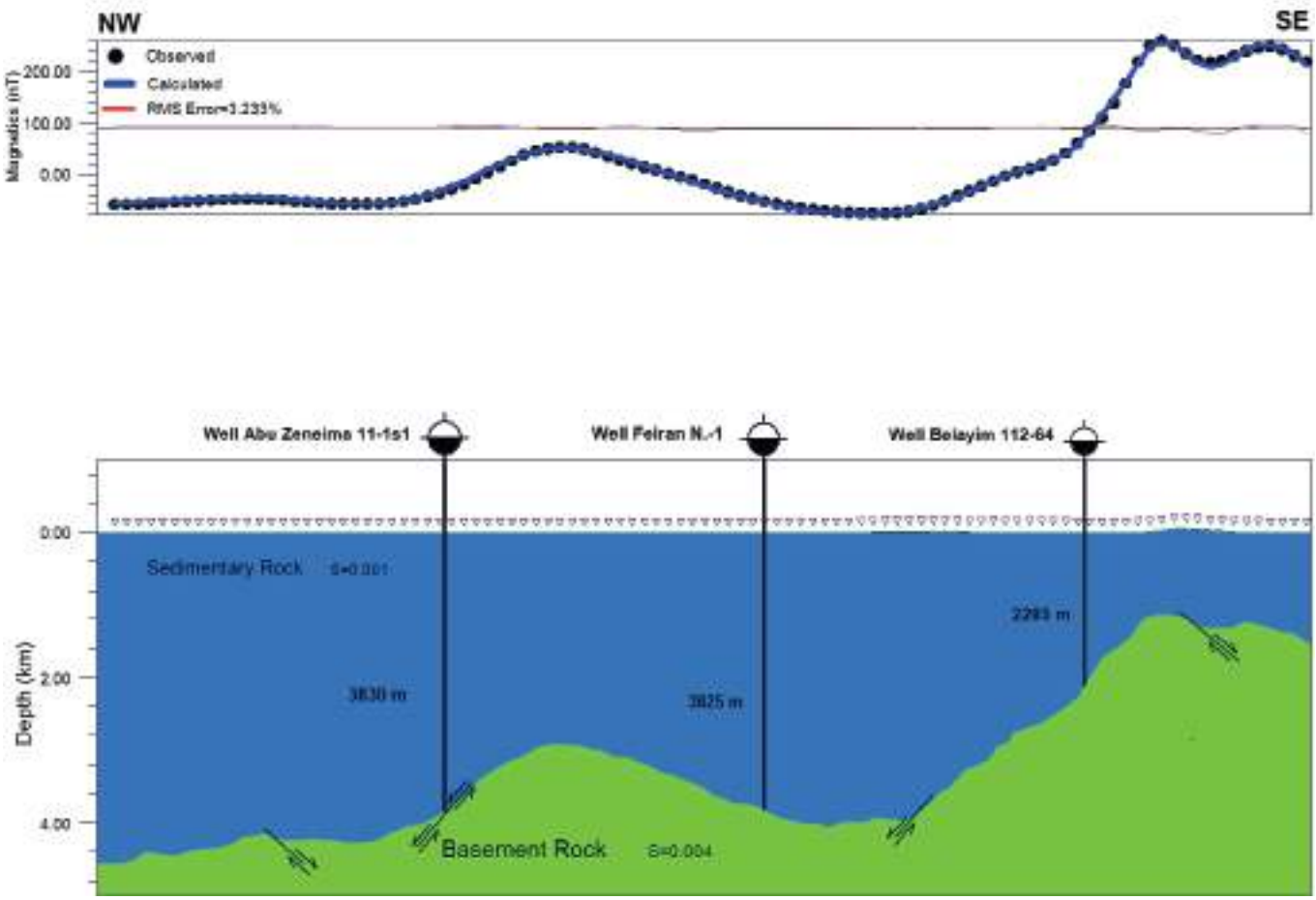

Figure 8. 2D inverted susceptibility layered-earth model and calculated geomagnetic response of the profile C, eastern part of the Gulf of Suez, Egypt.
Рисунок 8. Двухмерная модель магнитной восприимчивости, полученная решением обратной задачи для слоистой земли, и вычисленный геомагнитный отклик профиля С (восточная часть Суэцкого залива, Египет).

Conclusion

High-resolution airborne geomagnetic anomaly data sets were consistently and extensively acquired, processed and multi-dimensionally inverted over the eastern part of the Gulf of Suez. The starting models for all inversion trails were initially built-up using a priori information gained from the progressive standard qualitative and semi-qualitative interpretations. Three methods (AS, SPI and Euler) were applied to determine the depth to the basement. The results of the three methods were close to each other. The three maps showed two major zones in the area. The first zone in the western part of the area is characterised by high depth to basement. The second zone in the eastern part of the area has a depth to basement lower than the eastern part. The depth to the basement varies from 150 m to 5200 m. 2D inverted susceptibility layered-earth model was applied along three profiles within the area. The well data controlled the geometry and physical parameters of the basement blocks. Using GM–SYS–3D inversion code, 3D modelling was applied. Several inversion trials were gradually set with different susceptibility (Δk) between 0.035 and 0.08 SI during the inversion run. The effective susceptibility contrast was found close to the susceptibility contrast of 0.0628 SI. The depth to the basement correlated with the available drilled stratigraphic-control wells within the area under study. The depth to the basement in the area reliably varied between 10 and 4800 m from the existing averaged ground surface. The encountered basement relief at the study area was shown up with three major basinal structures. These basins are located at the north western, central western and south eastern parts of the area. The results suggest that the sedimentary cover is tectonically affected by deep-seated basement structures with a set of tectonic faults extending from the basement upwards through the

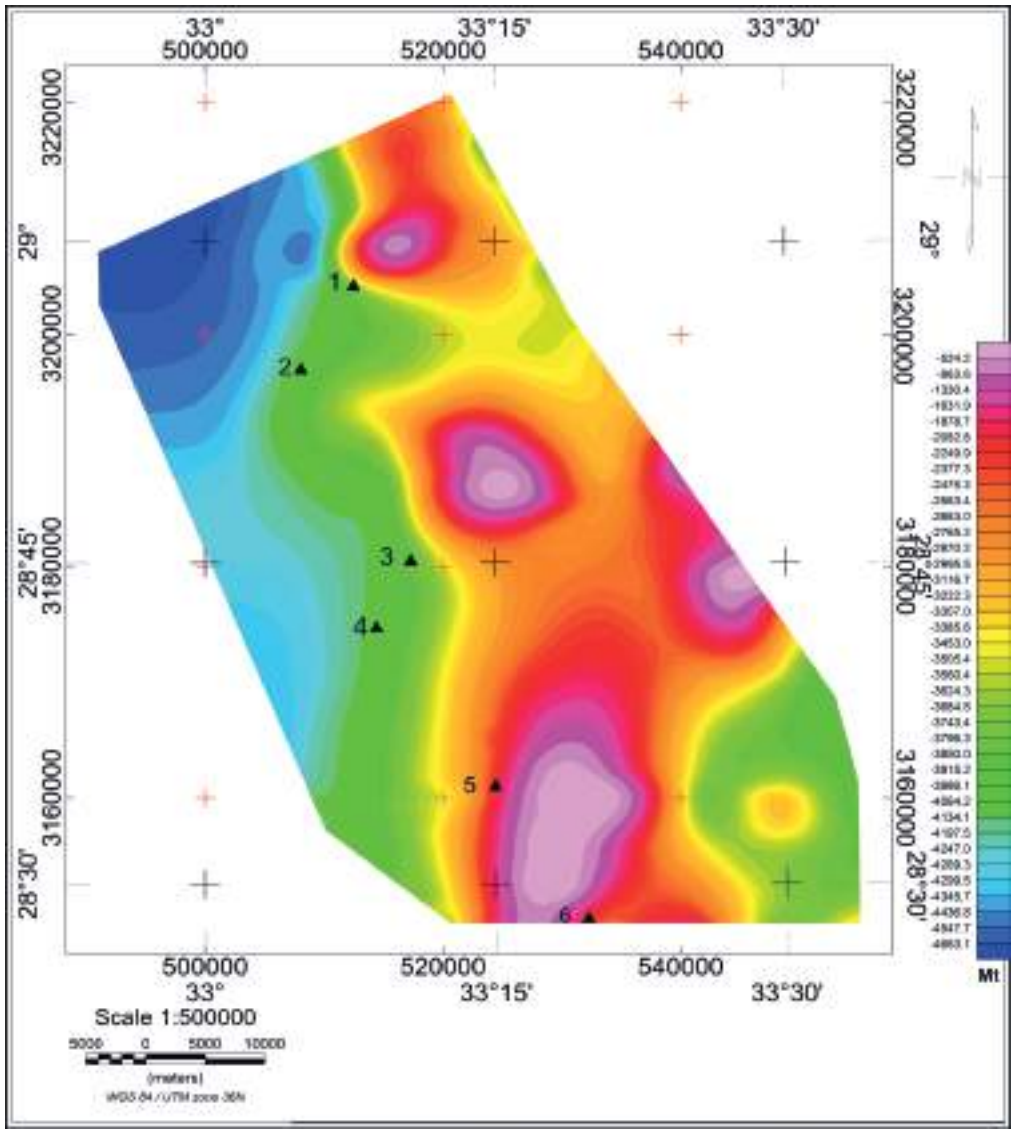

Figure 9. Basement relief contour map after performing the 3D layered-earth inversion of the subsurface magnetic susceptibility distributions and location of wells illustrated with numbers on the map, eastern part of the Gulf of Suez, Egypt.
Рисунок 9. Контурная карта рельефа фундамента после выполнения инверсии трёхмерной слоистой земли для распределения подповерхностной магнитной восприимчивости и расположение скважин, показанных цифрами на карте (восточная часть Суэцкого залива, Египет).

sedimentary cover. These faulted sedimentary blocks may constitute potential structural traps for the hydrocarbon accumulation; therefore further geophysical investigation could be needed.

REFERENCES

1. Meshref W. M. 1990, Tectonic framework of Egypt. In: R. Said (Ed.). The Geology of Egypt. Rotterdam, Netherlands, Balkema Publishers, pp. 113–156.
2. McClay K. R., Nicols G. J., Khalil S. M., Darwish M., Bosworth, W. 1998, Extensional tectonics and sedimentation, eastern Gulf of Suez, Egypt. In: B. H. Purser and D. W. I. Bosence (Eds.). Sedimentation and Tectonics of Rift Basins: Red Sea–Gulf of Aden. London, Chapman and Hall, pp. 223–238.
3. Dobrin M. B. 1976, Introduction to geophysical prospecting. N. Y., USA, McGraw-Hill Book Co. 630 p.
4. 2006, Geosoft. Montaj Geophysics Levelling System, Processing and enhancement geophysical data expansion for Oasis montaj. Toronto, Geosoft Inc. Vol. 3.
5. Kearey P., Michael B. 1994, An introduction to geophysical exploration. Second Edition. London, Great Britain, Blackwell Scientific Publication, p. 245.
6. Blakely R. J. 1995, Potential theory in gravity and magnetic applications. Cambridge, England, Cambridge University Press. 461 p.
7. Ali M. M. 2009, Acquisition, processing and interpretation of airborne magnetic and gamma-ray spectrometry survey data of Elkharga area, Central Western Desert Egypt, M. Sc. Thesis. Al Minufiya, Egypt, Menoufiya University, pp. 30–39.
8. Thurston J. B., Smith R. S. 1997, Automatic conversion of magnetic data to depth, dip, and susceptibility contrast using the SPI(TM) method. *Geophysics*. Vol. 62, pp. 807–813. https://doi.org/10.1190/1.1444190
9. Roest W. E., Verhoef J., Pilkington M. 1992, Magnetic interpretation using 3D analytic signal. *Geophysics*, vol. 57, pp. 116–125. https://doi.org/10.1190/1.1443174
10. Thompson D. T. 1982, EULDPH: A new technique for making computer-assisted depth estimates from magnetic data. *Geophysics*, vol. 47, pp. 31–37. https://doi.org/10.1190/1.1441278

11. Reid A. B., Allsop J. M., Granser H., Millet A. J., Somerton I. W. 1990, Magnetic interpretation. *Geophysics*, vol. 55, pp. 80–91. https://doi.org/10.1190/1.1442774
12. Rabeh T., Khalil A. 2014, Characterization of fault structures in southern Sinai Peninsula and Gulf of Suez region using geophysical data. *Environmental Earth Sciences*, vol. 73, pp. 1925–1937. https://doi.org/10.1007/s12665-014-3541-x
13. Attia H. M., Ahmed M. A., Korrat I. M. 2015, Thermal maturation simulation and hydrocarbon generation of the Turonian Wata formation in Ras Budran oil field, Gulf of Suez, Egypt. *Journal Environmental Sciences*, vol. 44, pp. 57–92.
14. Afife M. M., Al-Atta M. A., Ahmed M. A., Issa G. I. 2016, Thermal maturity and hydrocarbon generation of the Dawi Formation, Belayim Marine Oil Field, Gulf Of Suez, Egypt: A 1D basin modeling case study. *Arabian Journal of Geosciences*, vol. 9, pp. 1–31. https://doi.org/10.1007/s12517-016-2320-2
15. Azab A. A., El-khadragy A. A. 2013, 2.5-D gravity/magnetic model studies in Sahl El Qaa Area, Southwestern Sinai, Egypt. *Pure and Applied Geophysics*, vol. 170, pp. 2207–2229. https://doi.org/10.1007/s00024-013-0650-5

The article was received on December 12, 2018

УДК 550.83 https://doi.org/10.21440/2307-2091-2019-1-7-17

Методы изучения глубинного строения фундамента на основе аэромагнитных данных в восточной части Суэцкого залива, Египет

Сергей Владимирович ШИМАНСКИЙ[1, *],
Ахмед ТАРШАН[1, 2, **]

[1]Санкт-Петербургский государственный университет, Санкт-Петербург, Россия
[2]Управление ядерных материалов, Каир, Египет

Одним из лучших методов определения структур и строения фундамента является аэромагнитная разведка.
Целью данного исследования является точное определение глубинного строения фундамента и структур. Создание геофизических карт после обработки данных (включая двухмерные (2D) и трехмерные (3D) модели слоистой среды с магнитной восприимчивостью для RTP-магнитных данных высокого разрешения над восточной частью Суэцкого залива) проводилось с целью более точного определения неглубоких и глубоко расположенных структур фундамента. Для корреляции и контроля глубины фундамента во время 2D и 3D-моделирования использовались скважинные данные.
Результаты оценки глубины до фундамента показали, что метод налитического сигнала (AS), метод изображения источникового параметра (SPI) и метод Эйлера дают очень похожие результаты. Восточная часть на трех картах указывает на небольшие глубины, которые в некоторых местах достигают 300 м; с другой стороны, западная часть области указывает на большие глубины до фундамента, которые в других местах достигают 5000 м от существующего среднего показателя надземной поверхности. В расчетных и наблюдаемых данных трехмерное моделирование показало приемлемое соответствие от глубины до фундамента. На разрез осадочного чехла тектонически воздействуют такие глубоко расположенные структуры фундамента с множеством разломов, которые простираются от фундамента вверх через осадочный чехол. В целом эти нарушенные осадочные блоки могут формировать потенциальные структурные ловушки и накапливать углеводороды.

Ключевые слова: 2D и 3D магнитная восприимчивость, модели слоистой среды, глубинные структуры фундамента, региональные и аномальные, редуцированные к полюсу данные (RTP), восточная часть Суэцкого залива.

Статья поступила в редакцию 12 декабря 2018 г.

*s.shimanskii@spbu.ru
http://orcid.org/0000-0001-9710-9392
** ahmed_ramadan_geo@hotmail.com
http://orcid.org/0000-0002-5403-5220